

## Enhancement of Hydrothermally Co<sub>3</sub>O<sub>4</sub> Thin Films as H<sub>2</sub>S Gas Sensor by Loading Yttrium Element

Suhad A. Hamdan\*

Iftikhar M. Ali

Received 6/5/2018, Accepted 2/9/2018, Published 17/3/2019



This work is licensed under a [Creative Commons Attribution 4.0 International License](https://creativecommons.org/licenses/by/4.0/).

### Abstract

The gas sensing properties of Co<sub>3</sub>O<sub>4</sub> and Co<sub>3</sub>O<sub>4</sub>:Y nano structures were investigated. The films were synthesized using the hydrothermal method on a seeded layer. The XRD, SEM analysis and gas sensing properties were investigated for Co<sub>3</sub>O<sub>4</sub> and Co<sub>3</sub>O<sub>4</sub>:Y thin films. XRD analysis shows that all films are polycrystalline in nature, having a cubic structure, and the crystallite size is (11.7)nm for cobalt oxide and (9.3)nm for the Co<sub>3</sub>O<sub>4</sub>:10%Y. The SEM analysis of thin films obviously indicates that Co<sub>3</sub>O<sub>4</sub> possesses a nanosphere-like structure and a flower-like structure for Co<sub>3</sub>O<sub>4</sub>:Y.

The sensitivity, response time and recovery time to a H<sub>2</sub>S reducing gas were tested at different operating temperatures. The resistance changes with exposure to the test gas. The results reveal that the Co<sub>3</sub>O<sub>4</sub>:10%Y possesses the highest sensitivity around 80% at a 100°C operating temperature when exposed to the reducing gas H<sub>2</sub>S with 0.8sec for both recovery and response times.

**Key words:** Cobalt Oxide, H<sub>2</sub>S, Gas sensors, Sensitivity, Yttrium.

### Introduction:

Sensors play an essential part in the areas of environmental protection, emissions control, public safety, and human health (1). Research on metal oxide semiconductor (MOS) gas sensors has been ongoing for more than 50 years (2). It is well known that metal oxide has ultrahigh surface-to-volume ratios of materials that make their electrical properties sensitive to surface-adsorbed species and make them good candidates for gas sensing applications (1). MOS sensors are capable of detecting altered toxic or flammable gases for example, CO, NO<sub>2</sub>, CH<sub>4</sub> or VOC. Their procedure is based on the changes in electrical conductivity due to adsorption of reducing or oxidizing gases on MOS films. Commercially present semiconductor gas sensors are generally based on n-type thick films. Comparison to the n-type semiconductors, another from could be the p-type materials like Cr<sub>2</sub>O<sub>3</sub>, Cr<sub>2</sub>O<sub>3</sub>-TiO<sub>2</sub>, or Co<sub>3</sub>O<sub>4</sub>. With the latter material, the working temperatures are rather low (well under 300°C). An accurate physico-chemical model, describing the gas sensing mechanism, is one of the bases for such development work. A multiplicity of models exists which describe the gas response of n-type oxides because of their wide-scale application however there are less models for p-type ones.

Department of Physics, College of Science, University of Baghdad, Baghdad, Iraq.

\*Corresponding author: [suhadah22@gmail.com](mailto:suhadah22@gmail.com)

As in the case of n-type materials, the response of p-type materials to reducing gases is most commonly attributed to surface reactions with negatively charged ionosorbed oxygen species for example O<sup>-</sup> (3). The limitation of the application of p-type semiconductor oxides CuO, NiO, Co<sub>3</sub>O<sub>4</sub> etc. is chiefly as a result of their high electrical resistance and lower sensitivity to gases in dry air in comparison to n-type oxides (4).

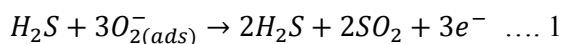
This work's reports are that of a gas sensor based on Cobalt oxide (Co<sub>3</sub>O<sub>4</sub>). It is a p-type semiconductor with a spinel structure. The Co<sup>2+</sup> ions occupy one-eighth of the tetrahedral sites and Co<sup>3+</sup> ions occupy half of the octahedral sites (5). Cobalt oxide has direct optical band gaps at 1.48 and 2.19 eV (6). Hydrothermal synthesis can be defined as a technique that depends on the solubility of minerals in hot environment under high pressure to obtain interested nanostructures where the crystal growth is achieved in a tool consisting of a steel pressure vessel called an autoclave (7).

Metal oxide surfaces are finished by oxygen species in air. Oxygen molecules on the surface of metal oxides gain electrons from the metal oxides and form oxygen ions. The metal oxide surfaces have a hole accumulation layer for the p-type and electron depletion layer for the n-type. When reductive gases are introduced, the thickness of the electron-depletion layer decreases. Thus, the resistance of n-type metal oxide gas sensor decreased. By

comparison, the resistance of p-type metal oxide gas sensors rises because of the decrease in the hole accumulation layer (8).

Sensitivity, response and recovery time are essential performance parameters for gas sensors. The sensitivity of conductometric sensors is defined as the ratio of the device's resistance when exposed to target species to that in ambient air. Response (recovery) time is defined as the time period required for the device to undergo resistance changing from 10% (90%) to 90% (10%) of the value in equilibrium upon exposure to an oxidizing (reducing) analyze (9).

Reducing gases are those, which act as electron donors while interacting with metal oxide surface. Through this interaction, reducing gases desorb or eliminate the chemisorbed oxygen ions and physisorbed hydroxyl ions from the metal oxide surface. The variation in the resistance of the material is used to detect the concentration of reducing gases such as SO<sub>2</sub>, CO, H<sub>2</sub>, NH<sub>3</sub>, H<sub>2</sub>S and C<sub>2</sub>H<sub>5</sub>OH by the chemical changes (10). On the metal oxide surface, H<sub>2</sub>S vapor powerfully reacts with the metals to form elemental sulfur. Oxygen adsorption on the metal oxide surface helps the response of H<sub>2</sub>S vapor, described in Eq.1 (11).



Eq.1 explains the strong reduction behavior that occurs in dense oxygen atmospheres along with the bi-product of sulfur dioxide and water vapor.

At low partial pressure of oxygen, H<sub>2</sub>S directly reacts with lattice oxygen to form SO<sub>4</sub> and yields the oxygen vacancy in the surface of the metal oxide which, in sequence, increases the conductance as given in Eq. 2(12)



where 5O<sub>0</sub><sup>x</sup> represents electrically neutral oxygen atoms in their lattice.

At nothing of oxygen in the atmosphere or after continuous interaction of H<sub>2</sub>S on the surface, adsorbed oxygen was totally desorbed and it led to direct interaction with the surface and resulted in the creation of elemental sulfur. This sulfur can replace the lattice oxygen and the obtained reaction is said to be sulfurization (13). In the current work, the gas sensing property of the film was improved significantly which may be due to the catalyst effect in the addition of yttrium nanoparticles in the structure of metal oxide.

In the present work, nanocrystalline Co<sub>3</sub>O<sub>4</sub> and Co<sub>3</sub>O<sub>4</sub>:Y was prepared through the hydrothermal method, and the structural, electrical, and sensing properties for H<sub>2</sub>S reducing gas have

been examined. The interaction of gas with films will be discussed. The temperature requirements of the sensor signal and the values of recovery time and response time have been calculated.

### Material and Methods:

Pure Co<sub>3</sub>O<sub>4</sub> and Co<sub>3</sub>O<sub>4</sub>:Y thin films have been prepared using the hydrothermal method onto a seeded layer. Firstly, to prepare the seeded layer, PVA (C<sub>4</sub>H<sub>6</sub>O<sub>2</sub>)<sub>n</sub> will be used, which dissolves in distilled water. The aqueous solutions of cobalt nitrate and Yttrium nitrate with 0.1M are stirred separately in magnetic stirrer for 10 min to prepare the precursors which are the sources of cobalt and yttrium ions. Then, a cobalt precursor is added to 1.5 g of PVA at 80°C for 2hours. This solution is irradiated with 2.4 GHz microwave frequency at power 220W for 10 min, then the pH for the solution was measured and its value was controlled at 8pH or until the color of the solution changed. The resultant solution has been spin coated onto silicon and glass substrates at 1500 rpm for 1min, this step was repeated several times to obtain the desired thickness for seed layer.

The above steps are for the preparation of pure seed layer solution. To prepare a seed layer solution with yttrium, the same steps have been taken but mixing two different salts, cobalt nitrate, and yttrium nitrate in a magnetic stirrer for 1 h at 70°C before adding a PVA solution. Finally, these seed layers have been dried at 120°C for a few minutes so as to achieve suitable adhesion of the seeded particles on the surface of the substrate. The chief purpose of using seed layer is to supply nucleation locations by weakening the thermodynamic barrier between heterogeneous materials. An additional advantage that has been detected is that when seed layer was used, the grown nanostructures were found to be well aligned, greatly dense and uniform. These seeded layers are thermal annealed at 210°C for 1h to remove the PVA, then annealed at 380°C for 2h to improve crystallinity and remove the hydroxide phase. Then, samples are prepared for the next step, which is growth process.

To prepare a growth solution, 0.1M cobalt nitrite (as a source of cobalt ions) and 0.1M Hexamine C<sub>6</sub>H<sub>12</sub>N<sub>4</sub> (as an oxidized agent) are dissolved separately in distilled water and stirred for 10 min. Then, these two solutions are mixed and stirred for 10 mins. For Co<sub>3</sub>O<sub>4</sub>:Y preparation, the same procedure is conducted, but before adding hexamine, yttrium nitrate (as a source of yttrium ions) is added to cobalt nitrate in an appropriate amount and stirred together at 70°C for 1h to permit these two elements to disperse well, and then after 1h hexamine is added. The mixture was transferred

into a Teflon-lined stainless-steel autoclave where the substrates with seeded layers are vertically

aligned inside the Teflon container as shown in fig. (1).

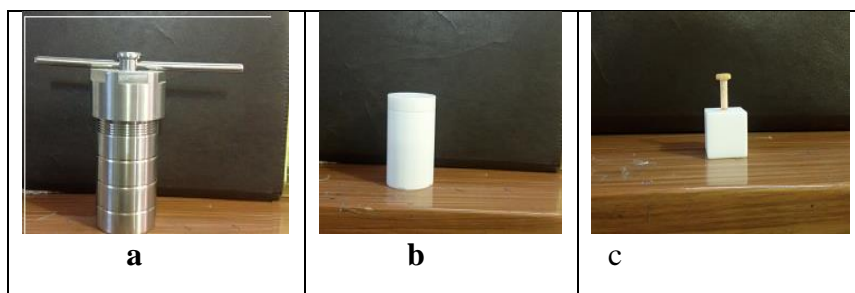


Figure 1. Photograph of a) an autoclave vessel Inner; b) a Teflon container; c) a Teflon sample holder

The autoclave was sealed with haste and kept at 100°C for 4h in a digital temperature-controlled oven. Then, the autoclave was cooled to room temperature naturally. The substrates are washed with distilled water to eliminate any residual solid particles from the surface or unreacted atoms, and then the samples are dried in oven at 100°C for 30 min. The annealing process will happen inside a furnace at 500°C for 1h to convert the hydroxide phase  $\text{Co}(\text{OH})_2$  into  $\text{Co}_3\text{O}_4$ . Therefore, the films are ready to be characterized.

The autoclave features a shell that is made of stainless steel (SS304), with temperature ranges between (100-300)°C, a capacity of 100ml, and a pressure of  $\leq 3\text{Mpa}$  (Toption Instrument Co. Limited, China).

An pure aluminum e finger-shaped metal contacts as electrodes with a thickness of 250nm were deposited on top of the  $\text{Co}_3\text{O}_4:\text{Y}$  thin films, using an E306A Edwards thermal evaporation system under high vacuum of  $10^{-5}$  mbar by rotary.

The testing of gas sensor is achieved using the setup shown in Fig. (2) that illustrated the schematic diagram of the electrical circuit for gas sensing measurements.

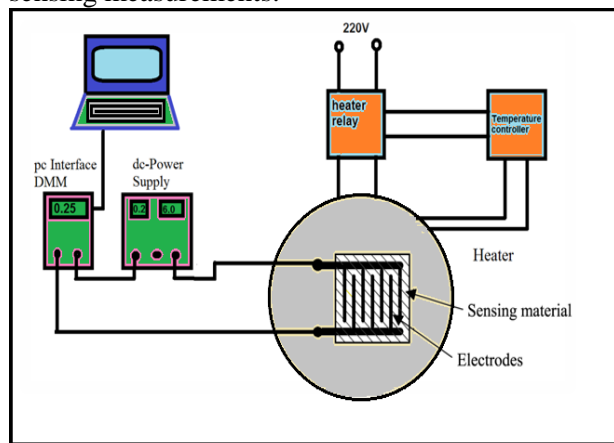


Figure 2. Schematic diagram of gas sensing and the electrical circuit setup.

The structural properties are determined by X-ray diffraction (XRD- 6000 Labx, supplied by

Shimadzu, X-ray source Cu). Film morphology was analyzed using a MIRA3 model – TE-SCAN, Field Emission Scanning Electron Microscope (FESEM) (Dey Peteronic Co. Tehran, Iran). Electrical properties such as Hall Effect and dc-measurement have been investigated and finally, sensing properties have been investigated. Experimental work is shown in the scheme of Fig. (3).

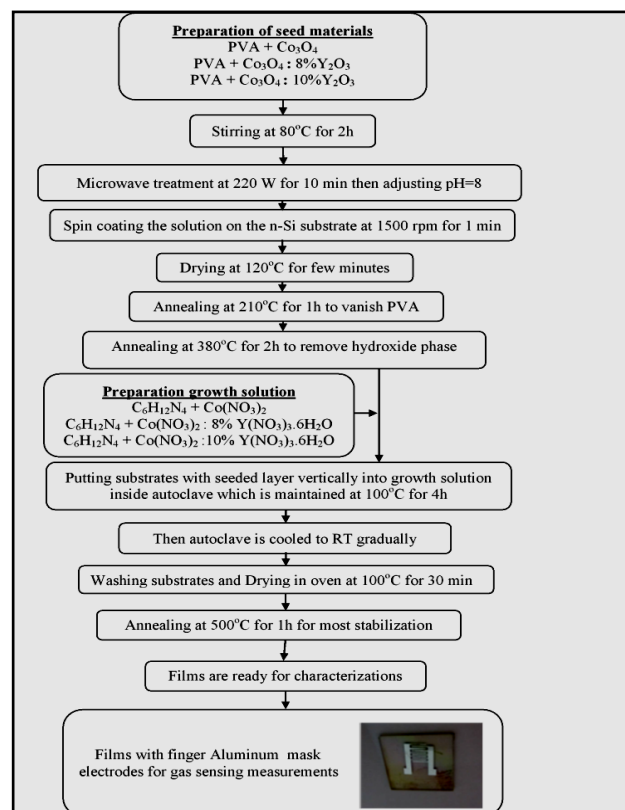


Figure 3. Flow diagram for  $\text{Co}_3\text{O}_4$  films prepared

## Results and Discussion:

The x-ray diffraction patterns of prepared cobalt oxide and cobalt yttrium oxide grown onto silicon substrates are displayed in fig. (4). It observed that the patterns exhibit diffraction peaks around ( $2\theta \sim 31.5044^\circ$ ,  $37.0796^\circ$ ,  $38.8496^\circ$ ,  $44.9558^\circ$ ,  $56.0177^\circ$ ,  $59.6460^\circ$  and  $65.3097^\circ$ ) referred

to as (202), (311), (222), (400), (422), (333), and (404) favorite directions respectively for cobalt oxide which is in agreement with (ASTM) card number 96-900-5888.

In addition to these peaks it is observed that the patterns exhibit diffraction peaks around (20~33.8230°, 48.7611° and 57.8200°) referred to as(400), (440), and (622) favorite directions respectively for yttrium oxide as shown in Table (1), which agrees with (ASTM) card number 96-100-9018. This proves the cubic structure for hydrothermally prepared cobalt oxide and illustrates the presence of a Co<sub>3</sub>O<sub>4</sub> phase and same peaks appeared with the researchers (14-16). Crystallite size is estimated by Scherer's formula equation (14):

$$D = \frac{K\lambda}{\beta \cos\theta} \dots\dots\dots 3$$

where β is the full width at half-maximum (FWHM) , θ is the angle of the diffraction peak, K is the shape factor (0.94), and λ is 0.15405 nm which is the wavelength of the x-ray source . The crystallite size D is 11.7 nm for cobalt oxide and it is 9.3 nm for cobalt yttrium oxide which means the size decreases by adding yttrium.

Lattice constant a is calculated by using the predominated orientation (311) from the following equation (14):

$$d_{hkl} = \frac{a}{\sqrt{h^2 + k^2 + l^2}} \dots\dots\dots 4$$

where hkl are miller indices and d<sub>hkl</sub> is interplaner spacing which is calculated using Bragg's law:

$$n\lambda = 2 d_{hkl} \sin\theta \dots\dots\dots 5$$

The calculated lattice constant of the cobalt oxide nanostructure grown on silicon was 8.0348Å and 7.998Å for Co<sub>3</sub>O<sub>4</sub>:Y nanostructure. Strain is calculated using the following relations (17) and (18):

$$s = \frac{a - a_0}{a_0} \times 100\% \dots\dots\dots 6$$

where a<sub>0</sub> is the standard lattice constant for an unstained cobalt oxide lattice which equals 8.084Å. The values of strain are -0.00609 and -0.01064 for cobalt oxide and cobalt yttrium oxide respectively. The negative value for strain is related to the compressive strain which is due to the nanosize effect.

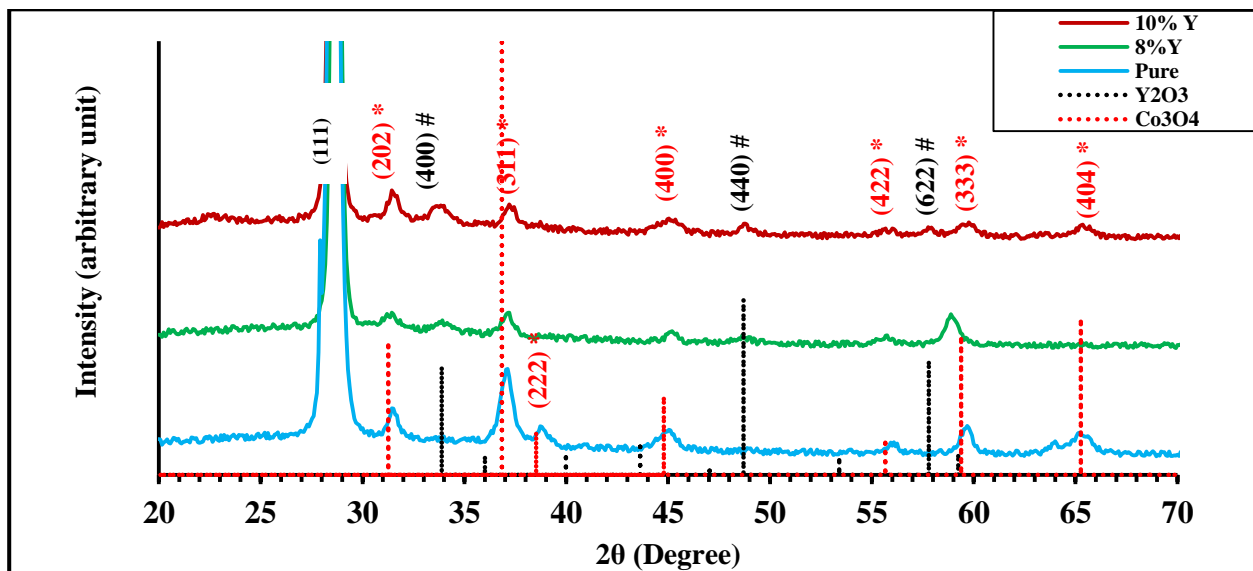


Figure 4. XRD patterns of Co<sub>3</sub>O<sub>4</sub> and Co<sub>3</sub>O<sub>4</sub>:Y grown onto Si substrates

Table (1) displays structural parameters calculated from XRD spectra for cobalt oxide and cobalt yttrium oxide. The existence of yttrium causes deformation or distortion to the Co<sub>3</sub>O<sub>4</sub>

lattice, which may be due to the large ionic radius of Y<sup>+3</sup> which equals 0.9 Å compared with that of Co<sup>+3</sup> which is 0.63 Å (19),

**Table 1. Structure Parameters for Co<sub>3</sub>O<sub>4</sub> and Co<sub>3</sub>O<sub>4</sub>:Y**

Sample	2θ (Deg.)	β (Deg.)	D (nm)	hkl	Phase	Card No.
Co <sub>3</sub> O <sub>4</sub>	31.5044	0.4	17.3	(202)	Co <sub>3</sub> O <sub>4</sub>	96-900-5888
	37.0796	0.7	11.7	(311)	Co <sub>3</sub> O <sub>4</sub>	96-900-5888
	38.8496	0.6	13.2	(222)	Co <sub>3</sub> O <sub>4</sub>	96-900-5888
	44.9558	1.03	8.3	(400)	Co <sub>3</sub> O <sub>4</sub>	96-900-5888
	56.0177	0.6	14.1	(422)	Co <sub>3</sub> O <sub>4</sub>	96-900-5888
	59.6460	0.63	14.4	(333)	Co <sub>3</sub> O <sub>4</sub>	96-900-5888
	65.3097	1.03	9.1	(404)	Co <sub>3</sub> O <sub>4</sub>	96-900-5888
	31.3442	2.8	9.3	(202)	Co <sub>3</sub> O <sub>4</sub>	96-900-5888
	33.8400	2.6	10.9	(400)	Y <sub>2</sub> O <sub>3</sub>	96-100-9018
	37.1049	0.8	10.5	(311)	Co <sub>3</sub> O <sub>4</sub>	96-900-5888
Co <sub>3</sub> O <sub>4</sub> :8% Y	45.1699	2	13.9	(400)	Co <sub>3</sub> O <sub>4</sub>	96-900-5888
	48.7100	1.8	11.8	(440)	Y <sub>2</sub> O <sub>3</sub>	96-100-9018
	55.6300	1.6	12.1	(422)	Co <sub>3</sub> O <sub>4</sub>	96-900-5888
	58.9069	1.5	12.9	(333)	Co <sub>3</sub> O <sub>4</sub>	96-900-5888
	31.5044	2.8	13.3	(202)	Co <sub>3</sub> O <sub>4</sub>	96-900-5888
	33.8230	2.6	8.5	(400)	Y <sub>2</sub> O <sub>3</sub>	96-100-9018
	37.2566	0.9	9.3	(311)	Co <sub>3</sub> O <sub>4</sub>	96-900-5888
	38.7611	2.3	15.9	(222)	Co <sub>3</sub> O <sub>4</sub>	96-900-5888
	45.0442	2.0	7.5	(400)	Co <sub>3</sub> O <sub>4</sub>	96-900-5888
	48.7611	1.8	12.3	(440)	Y <sub>2</sub> O <sub>3</sub>	96-100-9018
Co <sub>3</sub> O <sub>4</sub> :10% Y	55.7522	1.6	8.5	(422)	Co <sub>3</sub> O <sub>4</sub>	96-900-5888
	57.8200	1.59	11.3	(622)	Y <sub>2</sub> O <sub>3</sub>	96-100-9018
	59.6460	1.54	8.6	(333)	Co <sub>3</sub> O <sub>4</sub>	96-900-5888
	65.3982	1.4	10.7	(404)	Co <sub>3</sub> O <sub>4</sub>	96-900-5888

**Table 2. average strain and average crystallite size of Co<sub>3</sub>O<sub>4</sub> and Co<sub>3</sub>O<sub>4</sub>:Y**

Sample	s
Co <sub>3</sub> O <sub>4</sub>	-0.00508
Co <sub>3</sub> O <sub>4</sub> :8% Y	-0.00186
Co <sub>3</sub> O <sub>4</sub> :10% Y	-0.00523

SEM measurements were used to analyze the grain size and surface morphology of the seeded layers which were prepared using the spin coating technique and growth layer which were prepared using the hydrothermal method for Co<sub>3</sub>O<sub>4</sub> and cobalt yttrium oxide thin films. The seed layer and growth film of pure Co<sub>3</sub>O<sub>4</sub> nanoparticles showed the sphere like nanostructure which is in agreement with (14) as shown in fig.s 5a and 5b. The addition of yttrium to Co<sub>3</sub>O<sub>4</sub> influences the surface morphology sample; the structure transformed into to nanoflower which were observed to have been

deteriorations. The seed layer is illustrated in fig.s 5c and 5e for doping films with 8% Y and 10% Y respectively, while growth film is shown in fig.s 5d and 5f for doping films with 8% Y and 10% Y respectively. So, lattice deformation occurs upon yttrium addition.

The surface area to volume ratio (S/V) which plays important roles in the performance gas, the high (S/V) ratio was obtained by decreasing the size of the grains (20). Furthermore, morphology of the metal oxide influences the response as it changes the number of active sites for adsorption (10). Table (1) shows the average crystallite size was bigger for pure Co<sub>3</sub>O<sub>4</sub> than Co<sub>3</sub>O<sub>4</sub>: Y, this may be due to the change in structure from spherical to nanoflower shape; compressive strain increased with the addition of yttrium.

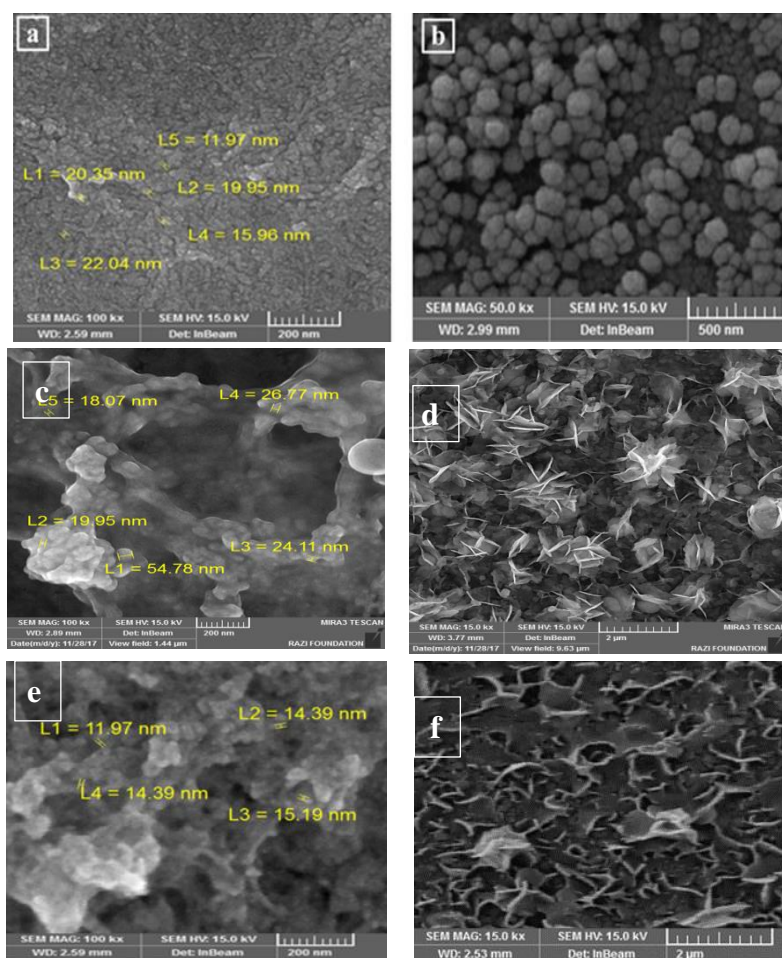


**Figure 5. SEM images of  $\text{Co}_3\text{O}_4$  nanoparticles: a) Seed layer for pure  $\text{Co}_3\text{O}_4$ , b) Growth layer for pure  $\text{Co}_3\text{O}_4$ , c) Seed layer for  $\text{Co}_3\text{O}_4:8\%\text{Y}$ , d) Growth layer for  $\text{Co}_3\text{O}_4:8\%\text{Y}$  e) Seed layer  $\text{Co}_3\text{O}_4:10\%\text{Y}$ , and f) growth layer  $\text{Co}_3\text{O}_4:10\%\text{Y}$ .**

The gas sensing property of the sensor is measured by variation in resistance over two sensing electrodes under  $\text{H}_2\text{S}$  gas. The sensitivity of the  $\text{Co}_3\text{O}_4$  and  $\text{Co}_3\text{O}_4:\text{Y}$  gas sensors toward  $\text{H}_2\text{S}$  reducing gas is determined using the following equation (21):

$$S(\%) = \left| \frac{R_g - R_a}{R_a} \right| \times 100 \dots \dots 7$$

where  $R_a$  and  $R_g$  are the resistances of the sensor in air atmosphere and in target gas, respectively. Figures (6a-i) and tables (3,4) show sensitivity, response and recovery times of pure cobalt oxide and Cobalt-Yttrium-Oxide to a  $\text{H}_2\text{S}$  gas sensor.

Additives can enhance gas sensitivity, as shown in fig. (6) and Table (3). A nonsystematic increase of gas sensitivity with yttrium addition to cobalt oxide result in high gas sensitivity equal to (14.0714%) when a 10% Y additive at temperature=150°C is exposed to  $\text{H}_2\text{S}$  reducing gas. This is in agreement with publicists' view that they are additives to metal oxides, which successfully

support their sensing features by lowering the energy essential for chemisorption of gas molecules on the semiconductor surface. Adding an appropriate amount of yttrium can stabilize a particular valence state and raise the electron exchange rate.

Consequently, the 10% Y sample has highest sensitivity due to having the smallest crystallite size (9.3 nm) as shown in Table (1). Reducing the crystallite size might have an effect on the width of the space charge region which assists the chemisorption of gas molecules and the sensing process. This is in agreement with Yamazoe et al. who have created a reverse relationship between grain size and the response. Also, a Co-Y- oxide with 10% Y has a smaller crystallite size and consequently has a high (S/V) ratio, so there is higher gas sensitivity.

Operating temperature limits the sensing performance and features of the thin film gas sensors as seen in fig. (6) and Table (3). From Table (3), it can be concluded that adding 8% Y to  $\text{Co}_3\text{O}_4$  and getting a maximum sensitivity where  $T=200^\circ\text{C}$  when increasing the Y ratio to 10% begets a higher

sensitivity at low working temperature 100°C. This means it is better to get a low working temperature

operation and high sensitivity. Table (4) shows the response time and recovery time.

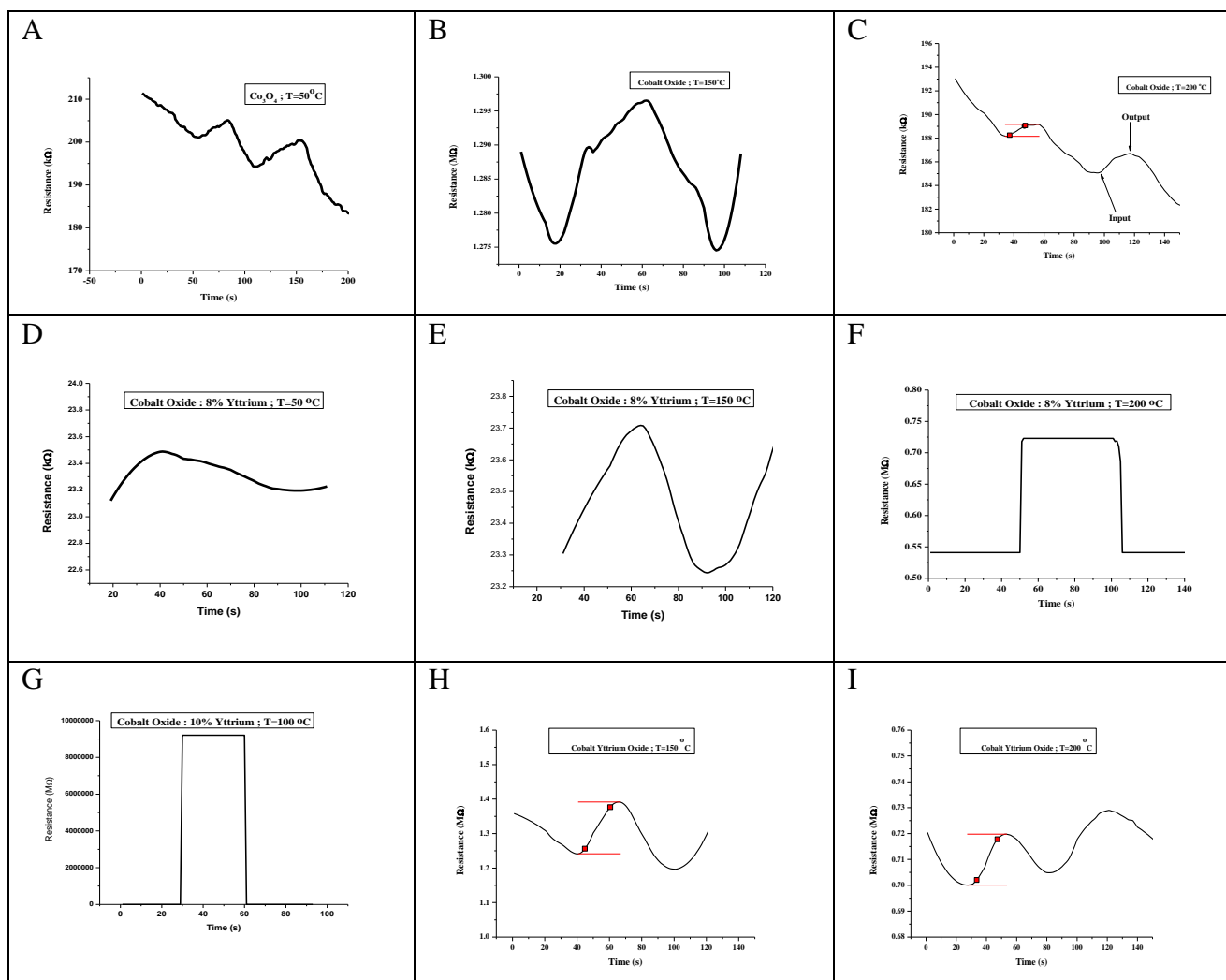


**Figure 6.** The difference in resistance with time for a H<sub>2</sub>S gas sensor with different operating temperatures; (a-c) for pure cobalt oxide; (d-f) for Co<sub>3</sub>O<sub>4</sub>:8%Y and (g-i) for Co<sub>3</sub>O<sub>4</sub>:10%Y.

The sensitivity improved by increasing the operating temperature for the reason that the operating temperature affects the receptor function (receptor function, the first phase of sensing occurrence, is a chemical procedure between goal gas in the air and metal oxide surface). The air is caused by its influence on the chemical dynamics on a gas-solid interface and thus limits essential sensing properties, for example response time, recovery time, response, selectivity, and stability. The property of the metal oxide strongly depends on the synthesis method and its preparation conditions.

Hence, the response of a metal oxide film in the direction of a particular gas strongly depends on the orientation of the crystal surface (10).

**Table 3. Sensitivity of Cobalt-Yttrium –Oxide H<sub>2</sub>S gas sensor**

%Y	Sensitivity % at				
	50 °C	100 °C	150 °C	200°C	250°C
0	2.6	-	2.15	2.21	---
8	1.52	--	3.09	24.65	0.11
10	0.13	88.4	14.07	5.58	1.73

**Table 4. Response and Recovery times for Cobalt-Yttrium–Oxide H<sub>2</sub>S gas sensor.**

%Y	Res. time (s) / Rec. time (s) at:				
	50 °C	100 °C	150 °C	200°C	250°C
0	22 /18.15	x / x	29.8 / 25.71	10.32 / 25.61	x / x
8	14.67 / 38.03	x / x	22.7 / 16.61	0.82 / 1.65	28.6 / 37.31
10	0.8 / 0.8	0.8 / 0.8	15.65 / 19.58	13.65 / 16.94	19.15 / 9.15

**Conclusions:**

This investigative report for  $\text{Co}_3\text{O}_4:\text{Y}$  Nano Structure thin film sensor was synthesized using the hydrothermal method on silicon n-type substrates. SEM images of  $\text{Co}_3\text{O}_4$  film show the structure to be sphere-like and  $\text{Co}_3\text{O}_4:\text{Y}$  is observed to have a nanoflower-like structure. In general, there is a rapid response to hazardous  $\text{H}_2\text{S}$  gas especially at temperatures less than  $50^\circ\text{C}$  where the response time is less than 2.5 sec. It was observed that  $\text{Co}_3\text{O}_4:10\%\text{Y}$  has smallest crystallite size and grain size so that demonstrates good sensitivity value to  $\text{H}_2\text{S}$  gas with a fast response time and recovery time especially at  $100^\circ\text{C}$  operating temperature where its sensitivity was more than 80 % with 0.8 sec for both response and recovery times.

**Acknowledgment**

I am grateful to the staff of thin film laboratory in Dept. of Phys., College of Science, University of Baghdad for providing the necessary facilities and assistance to complete this work non conflicts of interest.

**Conflicts of Interest: None.****References:**

- Shelke P, Datir A, Chakane S, Mohite K, Adsool A. Use of Cobalt Oxide in an Ammonia Gas Sensor Operating at room Temperature. *EEMIR*.2009 Apr - Dec.; 2(5-6):63-71.
- Neri G. First Fifty Years of Chemosensitive Gas Sensors. *Chemosensors*. 2015 Jan; 3(1): 1–20.
- Kärkkäinen I, Floren A, Mändar H, Avarmaa T, Jaaniso R. Modelling and Characterisation of  $\text{Co}_3\text{O}_4$  Thin Film Gas Sensors. *Procardia Chem*.2009; 1: 654-657.
- Xu J m, Chenge J P. The advances of  $\text{Co}_3\text{O}_4$  as gas sensing materials A review. *J Alloys Compd*.2016; 686: 753-768.
- Vetter S, Haffer S, Wagner T, Timann M. Nanostructured  $\text{Co}_3\text{O}_4$  as a CO gas sensor: Temperature dependent behavior. *Sens Actuators B*.2015; 206:133-138.
- Jogade S M, Sutrave D S, Patil V B. Structural and Morphological Properties of Mn-Doped  $\text{Co}_3\text{O}_4$  Thin Film Deposited by Spin Coat Method. *IJERA*.2016 Sept; 6 (9):42-46.
- Zhu X , Hou K, Chen C , Zhang W, Sun H , Zhang G A et.al.. Structural-controlled synthesis of polyaniline nanoarchitectures using hydrothermal method. *High Perform Polym*.2015; 27(2): 207–216.
- Hübner M, Simion C, Tomescu A, Pokhrel S, Bârsan N, Weimar U. Influence of humidity on CO sensing with p-type CuO thick film gas sensors. *Sens Actuators B* .2011; 153: 347–353.
- Sounder J, Gowthaman P, Venkatachalam M, Saroja M. A Review of Gas Sensors Based on Semiconducting Metal Oxide. *IOSR-JEEE*. 2017 (Mar – Apr); 12(2):47-54.
- Shankar P, Bosco J. Gas sensing mechanism of metal oxides the role of ambient atmosphere type of semiconductor and gases A review. *Science Jet*.2015; 4(126):1-18.
- Xu J, Wang X, Shen J. Hydrothermal synthesis of  $\text{In}_2\text{O}_3$  for detecting  $\text{H}_2\text{S}$  in air. *Sens Actuators B*. 2006 Jun; 115(2):642-646.
- Capehart T W, Chang S C. The interaction of tin Oxide films with  $\text{O}_2$ ,  $\text{H}_2$ ,  $\text{NO}$ , and  $\text{H}_2\text{S}$  .*JVST*.1981Mar; 18(2):393.
- Kumar R, Khanna A, Sastry V. Interaction of reducing gases with tin Oxide films prepared by reactive evaporation techniques. *Vacuum*.2012 Mar; 86(9):1380-1386.
- Manickam M, Ponnuswamy V, Sankar C, Suresh R, Mariappan R, Chandrasekaran J. The Effect of Solution pH on the Properties of Cobalt Oxide Thin Films Prepared by Nebulizer Spray Pyrolysis Technique. *Int J Thin Fil Sci Tec*.2016; 5(3), 155-161.
- Wadekar K, Nemade K, Waghuley S. Chemical synthesis of cobalt oxide ( $\text{C}_3\text{O}_4$ ) nanoparticles using Co-precipitation method. *Res J Chem Sci*. 2017 Jan.; 7(1):53-55.
- Kerli S. Synthesis, Characterization and Supercapacitive Performances of Yttrium Doped Cobalt. *J Korean Phys Soc*. 2017 Oct; 71(7):404-407.
- Hassan J, Mahdi M, Ramizy A, Abu Hassan H, Hassan Z. Fabrication and Characterization of ZnO nanorods/P6H-Sic heterojunction LED by microwave-assisted chemical bath deposition. *Superlattices Microstruct*.2013; 53: 31-38.
- Sabah M, Hassan Z, Naser M, Al-Hardan NH, Bououdina M. Fabrication of low cost uv photo detector using ZnO nanorods grown on to nylon. *J Mater Sci Mater Electron*.2015; 26(3), 1322-133.
- Yi L, Hai-Jin L, Qing L, Hou-Tong L. Electrical transport and thermoelectric properties of Ni-doped perovskite-type  $\text{YCo}_{1-x}\text{Ni}_x\text{O}_3$  ( $0 \leq x \leq 0.07$ ) prepared by sol-gel process. *Chin Phys B* .2013; 22(5): 057201.
- Wang C, Yin L , Zhang L, Xiang D, Gao R. Metal Oxide Gas Sensors: Sensitivity and Influencing Factors. *Sensors*. 2010 Mar; 10:2088-2106.
- Ivanovkaya M. Gas-sensitive properties of thin film heterojunction based on  $\text{In}_2\text{O}_3$  nanocomposites. Elsevier Science. 2003; 7031, 1-9.

تحسين اغشية رقيقة  $\text{Co}_3\text{O}_4$  مائيا حراريا كمتحسس لغاز  $\text{H}_2\text{S}$  عن طريق تحميل عنصر الإيتريوم

افتخار محمود علي

سهاد عبد الكريم حمدان

قسم الفيزياء، كلية العلوم، جامعة بغداد، بغداد، العراق.

## الخلاصة:

تمت دراسة الخصائص التحسسية للاغشية  $\text{Co}_3\text{O}_4$  و  $\text{Co}_3\text{O}_4$ : Y النانوية. تم تحضير هذه الاغشية بطريقة مائية حرارية على طبقة البذرة. تم فحص الاشعة السينية XRD ومجهر المسح الالكتروني SEM وخصائص تحسسية الغاز درست للاغشية  $\text{Co}_3\text{O}_4$  و  $\text{Co}_3\text{O}_4$ : Y النانوية. فحص XRD يظهر كل الافلام متعددة التبلور و تمتلك تركيب مكعب ومعدل الحجم البلوري لاوكسيد الكوبلت النقي 11.7 نانومتر ولاوكسيد الكوبلت المطعم  $\text{Co}_3\text{O}_4$ :10% Y 9.3 نانومتر. تحليل المجهر الالكتروني الماسح SEM تشير بوضوح الى  $\text{Co}_3\text{O}_4$  تمتلك تركيب كروي و  $\text{Co}_3\text{O}_4$ : Y تمتلك تركيب نانوي يشبه الزهرة. تم اختبار التحسسية وزمن الاستجابة وزمن الاسترجاع للغاز المختزل  $\text{H}_2\text{S}$  في درجات حرارة تشغيل مختلفة. المقاومة تتغير نتيجة التعرض الى غاز الاختبار. النتائج اظهرت  $\text{Co}_3\text{O}_4$ :10% Y تمتلك اعلى تحسسية حوالي 80% في درجة حرارة تشغيل 100 درجة مئوية عند التعرض للغاز المختزل  $\text{H}_2\text{S}$  وزمن استجابة واسترجاع 0.8 ثانية.

الكلمات المفتاحية: كوبلت اوksيد،  $\text{H}_2\text{S}$ ، متحسسات الغاز، التحسسية، يتريوم .